Slowing of Sodium Channel Opening Kinetics in Squid Axon by Extracellular Zinc

WM. FRANK GILLY and CLAY M. ARMSTRONG

From the Marine Biological Laboratory, Woods Hole, Massachusetts 02543; and the Department of Physiology, University of Pennsylvania School of Medicine, Philadelphia, Pennsylvania 19104

ABSTRACT The interaction of Zn ion on Na channels was studied in squid giant axons. At a concentration of 30 mM Zn^{2+} slows opening kinetics of Na channels with almost no alteration of closing kinetics. The effects of Zn^{2+} can be expressed as a "shift" of the gating parameters along the voltage axis, i.e., the amount of additional depolarization required to overcome the Zn^{2+} effect. In these terms the mean shifts caused by 30 mM Zn^{2+} were +29.5 mV for Na channel opening (ON) kinetics ($t_{1/2}$ ON), +2 mV for closing (OFF) kinetics (τ_{OFF}), and +8.4 mV for the g_{Na}-V curve. Zn^{2+} does not change the shape of the instantaneous I-V curve for inward current, but reduces it in amplitude by a factor of ~0.67. Outward current is unaffected. Effects of Zn^{2+} on gating current (measured in the absence of TTX) closely parallel its actions on g_{Na}. ON gating current kinetics are shifted by +27.5 mV, OFF kinetics by +6 mV, and the Q-V distribution by +6.5 mV. Kinetic modeling shows that Zn^{2+} slows the forward rate constants in activation without affecting backward rate constants. More than one of the several steps in activation must be affected. The results are not compatible with the usual simple theory of uniform fixed surface charge. They suggest instead that Zn^{2+} is attracted by a negatively charged element of the gating apparatus that is present at the outer membrane surface at rest, and migrates inward on activation.

INTRODUCTION

Divalent cations affect the generation of action potentials, but the mechanisms involved are not yet entirely understood. Probably the most well known example is the action of Ca^{2+} on Na channels in the squid giant axon. In voltage-clamp experiments, Frankenhaeuser and Hodgkin (1957) showed that for a given depolarization fewer channels opened, and opened more slowly, in high Ca^{2+} than in normal sea water. Upon repolarization, the channels closed more rapidly in high Ca^{2+}. These effects were summarized with a simple and useful rule: raising the external Ca^{2+} concentration fivefold is roughly equivalent to hyperpolarizing the membrane by 15 mV. This idea has dominated

Address reprint requests to Dr. Wm. F. Gilly, Hopkins Marine Station of Stanford University, Pacific Grove, CA 93950.

J. GEN. PHYSIOL. © The Rockefeller University Press · 0022-1295/82/06/935/30 $1.00 935
Volume 79 June 1982 935-964

subsequent characterization of the effects of many other divalent cations, particularly the transition metals (see, for example, Hille et al., 1975; Arhem, 1980).

To explain the mechanism of calcium's action, Frankenhaeuser and Hodgkin followed a suggestion by A. F. Huxley and postulated that Ca^{2+} accumulates near negative charges, e.g., phospholipid head groups, fixed on the membrane's outer surface. The fixed charges electrostatically polarize the external medium and concentrate cations in an aqueous layer several angstroms thick next to the membrane. Divalent cations are attracted more strongly than monovalents, and enrichment of cations effectively "neutralizes" the negative surface charge. Electrical influence of the fixed surface charges and adjacent counterions spreads into the membrane and influences the gating apparatus of the ionic channels. Altering surface charge density by changing the divalent cation concentration is therefore proposed to change, or bias, the electric field sensed by the gating apparatus.

Several more detailed treatments of the fixed surface charge theory have been presented (Quincke, 1861; Chandler et al., 1965; Gilbert and Ehrenstein, 1969; Cole, 1969; McLaughlin et al., 1971; Brown, 1974; D'Arrigo, 1978). It is worth pointing out that although there is evidence for negative charges on membranes (Segal, 1968), there is no independent evidence for fixed charges that are near enough to the channels to influence their behavior. Such charges are theoretical constructs invoked only to explain the action of divalent cations on the channels.

If the hypothetical surface charges were uniformly or regularly distributed, changing the surface potential by adding Ca^{2+} would be, to a channel's gating apparatus, indistinguishable from a hyperpolarizing change in membrane voltage. This is a fundamental prediction of the theory. Thus, it is said that changing Ca^{2+} shifts the gating parameters along the voltage axis, and that raising Ca^{2+} shifts them to the right. The criterion for fulfilling this prediction is that divalent cations should perturb or shift opening rates, closing rates, and the steady state conductance-voltage relation by identical bias voltages. This criterion has not been satisfied for any biological membrane system.

One major discrepancy between published results and theory concerns the unusually large effect of certain divalent cations on the opening kinetics of Na (and K) channels. Dodge (1961) first showed that Ni ions drastically slowed the rate at which Na current (I_{Na}) developed in frog node while shifting the conductance-voltage relation very little (see also Hille, 1968). Qualitatively similar results have been reported for other polyvalent metal ions (Takata et al., 1966; Arhem, 1980).

A second difficulty concerns the theoretically equal effects of divalent cations on channel opening and closing rates; this has never been verified experimentally. Although Frankenhaeuser and Hodgkin (1957) found that high Ca speeded closing of Na channels, quantitative interpretation of this result in terms of surface charge theory is equivocal. Calcium ions are now known to enter open Na channels, particularly at negative voltages, and impede Na influx (Woodhull, 1973; Taylor et al., 1976). Effects of high

external Ca^{2+} on Na inactivation also fail to support the fixed surface charge theory (Shoukimas, 1978).

An obvious alternative to the simple fixed surface charge hypothesis, which we explore here, is the idea that the Na channel gating charge itself polarizes the medium next to the membrane and interacts with cations there.

This paper is the first of two describing the effects of zinc (II), a divalent transition metal cation, on activation of Na and K channels in squid axon. The effects of Zn^{2+} are not compatible with the uniform fixed surface charge hypothesis. Our results suggest that negative gating charges reside at the membrane's outer surface at rest, where they interact with Zn ions, thus stabilizing the resting state. We further suggest that this negative charge migrates inward during activation, generating a transient outward gating current.

Some of these results have appeared in preliminary form (Armstrong and Bezanilla, 1975; Armstrong and Gilly, 1979; Gilly and Armstrong, 1980*a* and *b*, 1981).

METHODS

All experiments were performed on cleaned, internally perfused axons of *Loligo pealei* at the Marine Biological Laboratory, Woods Hole, MA. The voltage clamp, electrodes, chamber, and computer data acquisition system were identical to those described in detail previously (Armstrong and Gilly, 1979).

External solutions contained either 0 or 116 mM NaCl, 10–15 mM $CaCl_2$, and 540 mM (for 0 Na) or 424 mM (for 116 Na) Tris 7.0 (Sigma Chemical Co., St. Louis, MO). 0 Na was used for measuring gating current (I_g), and 116 Na was used for I_{Na}. pH was 7.0–7.2. Zinc-containing solutions at this pH required isosmotic replacement of some Tris 7.0 with Tris free base. A ratio of Tris base to Tris 7.0 of 0.04:1.0 proved suitable; the final Tris concentrations were ~23.9 mM base and 471 mM 7.0 for 0 Na plus 30 Zn, and 17.9 mM base and 353 mM 7.0 for 116 Na plus 30 Zn. Only results with 30 mM $ZnCl_2$ are reported in this paper. This concentration is close to the solubility limit at pH 7, and a single experiment with 50 mM $ZnCl_2$ showed no obviously greater effects.

The internal solution normally used contained 150 mM tetramethylammonium (TMA) glutamate, 50 mM TMA-fluoride, 10 mM Tris 7.0, and sufficient sucrose to maintain osmolality at 1,040 mosmol/kg. For one experiment (Fig. 5B) 20 mM Na glutamate was added to this solution.

Usually I_{Na} (plus I_g) was recorded first in 116 Na ± 30 Zn (i.e., with or without 30 Zn). The measurements were then repeated in 0 Na ± 30 Zn to measure I_g alone. I_{Na} traces were subsequently generated by subtraction of the appropriately scaled 0 Na record from the 116 Na one. Tetrodotoxin (TTX) was not routinely used for I_g measurements (except in conjunction with Figs. 6 and 11). The reason, which will be discussed in this paper, involves an antagonism between Zn^{2+} and TTX. To minimize contamination of I_g records by residual ionic currents through Na channels, both ends of the fiber in the air gaps outside the guard regions of the chamber were carefully washed with the appropriate 0 Na solution. If this precaution was taken, and sufficient time was allowed to wash out internal K completely, acceptable I_g records were obtained (see also Results).

Linear ionic and capacity currents were removed from all traces with the P/4 procedure (Armstrong and Bezanilla, 1974) with control pulses taken at a very

negative voltage as indicated in the figure legends. Baselines for I_{Na} ON traces were fit to the points preceeding the pulse; those for I_{Na} OFF and all I_g traces were fit to points at the end of the sampling period. Normally I_{Na}, and occasionally I_g, was measured using compensation for 1 ohm·cm^2 of series resistance. Holding potential was −80 mV, and all experiments were performed at 8°C.

RESULTS

Na Channels Open Slowly but Close Normally in the Presence of Zinc

Fig. 1 summarizes the major effects of Zn^{2+} on Na channels. Fig. 1A shows I_{Na} (plus I_g) before, during, and after the application of Zn^{2+}. The important features are: (*a*) Na channels open more slowly in the presence of Zn^{2+} (I_{Na} ON), but (*b*) close normally after repolarization (I_{Na} OFF). (*c*) The peak current is smaller in Zn^{2+}. (*d*) These effects of Zn^{2+} are reversible, and nearly complete recovery occurred in this experiment. The data are from an axon in which inactivation was removed by internal pronase treatment (Armstrong et al., 1973), but Zn^{2+} acts identically in partially pronased (e.g., Fig. 2) or nonpronased (e.g., Fig. 13) axons. Pronase was routinely used in I_{Na} experiments in order to see activation kinetics uncomplicated by inactivation.

Kinetic effects (*a*) and (*b*) are better illustrated in Fig. 1B, in which the current trace recorded in Zn^{2+} has been scaled to match the maximum amplitude of the control current (average of the before and after records). Slowing of opening kinetics is obvious, whereas no change in closing kinetics is detectable.

Similar effects of Zn^{2+} are seen over the full voltage range of activation, as illustrated in Fig. 1C. I_g has been removed by subtraction in these records. For the depolarization to +50 mV, which should open nearly all the channels, ON kinetics are slowed, and steady state current in Zn^{2+} is 17% smaller than normal. At every other voltage I_{Na} is also slower and smaller in Zn^{2+}. There is a much greater decrease in steady state current produced by Zn^{2+} for small depolarizations, e.g., 67% at −30 mV.

The hypothetical bias voltage introduced by divalent cations that neutralizes fixed surface charge should slow opening (ON) kinetics, while accelerating the closing (OFF) rate. In addition, the equilibrium level of open channels achieved at any voltage should be perturbed by the identical bias voltage. Fig. 1 shows that such is not the case, and this conclusion is strengthened in the following sections.

Slowing of ON Kinetics by Zinc

Changes in ON kinetics of Na channels caused by Zn^{2+} are indicated in Fig. 2. In each set of records the dotted trace is I_{Na} in 30 mM Zn^{2+} at the indicated voltage, whereas the solid traces are control currents obtained at different voltages (see labels on Fig. 2) and scaled in amplitude to match the peak I_{Na} in Zn^{2+}. Comparison in this manner expresses the Zn^{2+} effect as the separation, or "shift," in millivolts of the control and Zn-modified currents that best superimpose.

As seen in Fig. 2, the shift in ON kinetics determined by superposition is not the same at all voltages. The Zn^{2+} trace at −30 mV (Fig. 2A) matches fairly

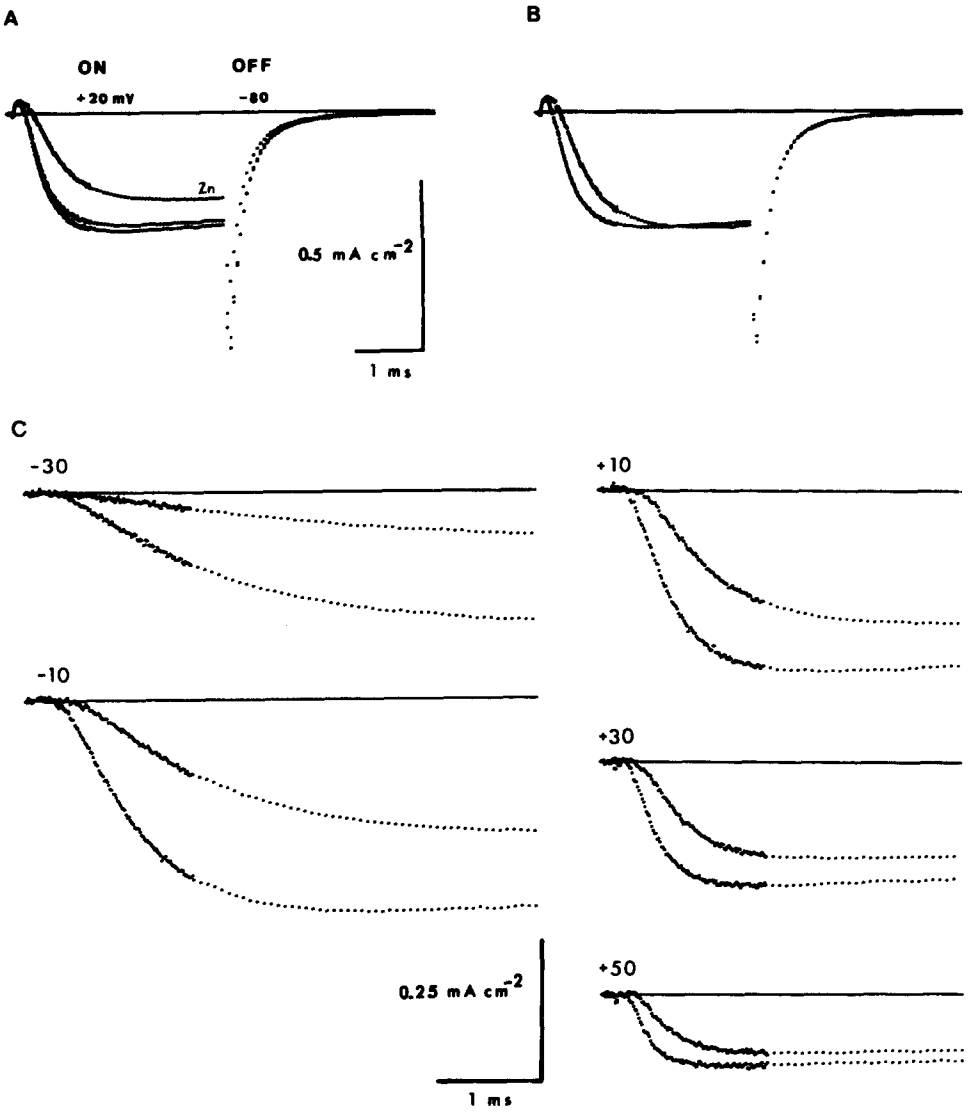

FIGURE 1. Effects of 30 mM $ZnCl_2$ in the presence of 12 mM $CaCl_2$ on I_{Na}. A. I_{Na} as Na channels open (I_{Na} ON) during a voltage-clamp depolarization to +20 mV and close (I_{Na} OFF) after repolarization to −80 mV. The trace of largest amplitude is control I_{Na} (I_g has not been subtracted out) in 116 Na. The smallest trace is I_{Na} in 116 Na + 30 Zn^{2+}. Recovery after Zn^{2+} exposure is shown by the middle trace. Inactivation of I_{Na} is greatly reduced due to internal pronase treatment at the beginning of the experiment. B. Zn^{2+} trace from left panel has been scaled 1.33× to match the peak control I_{Na} (average of before and after Zn from left panel). Slowing of ON kinetics is obvious; OFF rates are indistinguishable. C. I_{Na} in 116 Na ± 30 Zn^{2+} at a series of voltages as indicated. I_g has been removed by subtraction of the appropriate 0 Na records (see Methods). Smaller trace of each pair is that in Zn^{2+}. Same axon as in A, JN229B. Control pulses: P/4 from −120 mV.

well with the control trace at −40 mV, i.e., ON kinetics are shifted approximately +10 mV. The +60-mV trace in Zn^{2+} (Fig. 2D), however, superimposes with the control obtained at +20 mV, which indicates a shift of about +40 mV. At 0 mV (Fig. 2B) and +30 mV (Fig. 2C) the shifts are +10–20 mV and +20–30 mV, respectively.

OFF *Kinetics of* I_{Na} *Are Not Sensitive to Zinc*

Changes in closing kinetics produced by Zn^{2+} are much smaller than the effects on opening. Fig. 3 shows I_{Na} tails at various voltages after a pulse to 0

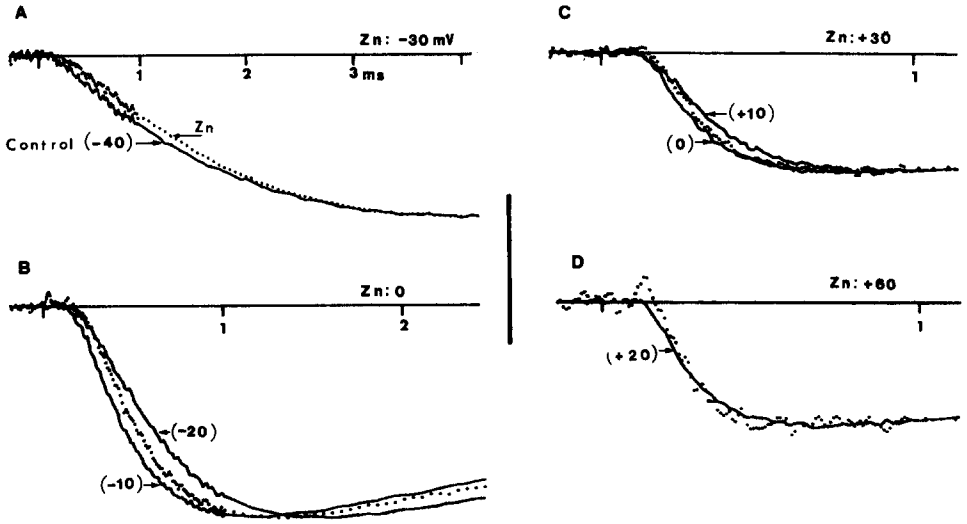

FIGURE 2. Superposition of I_{Na} ON traces recorded in 116 Na ± 30 Zn^{2+} at different voltages. In each figure, the zincked I_{Na} recorded at the indicated voltage is the dotted trace. Control I_{Na} recorded at more negative voltages as indicated in parentheses have been scaled to match the peak I_{Na} in Zn^{2+} and are plotted as the solid traces. The number of millivolts separating the Zn^{2+} and control traces that best superimpose increases steadily with increasing depolarization. Vertical I_{Na} scale bar represents in milliamperes per square centimeters: 0.05 (A), 0.50 (B), 0.25 (C), and 0.17 (D). Axon AU188C. Control pulses: P/4 from −120 mV.

mV. The Zn^{2+} trace is the dotted one in each set of records, and the scaled control records at three different voltages (see labels) are the solid ones. In all cases the Zn^{2+} and control traces nearly superimpose, indicating almost no change in the rate of channel closing.

Zinc Shifts the Steady State g_{Na}-*V Relation*

Sodium conductance was determined from tail current amplitude at −60 mV, as indicated in the inset to Fig. 4A. Current (I_{tail}) was read 50 μs after the return to −60 mV and adjusted as described in the figure legend. Thus, all

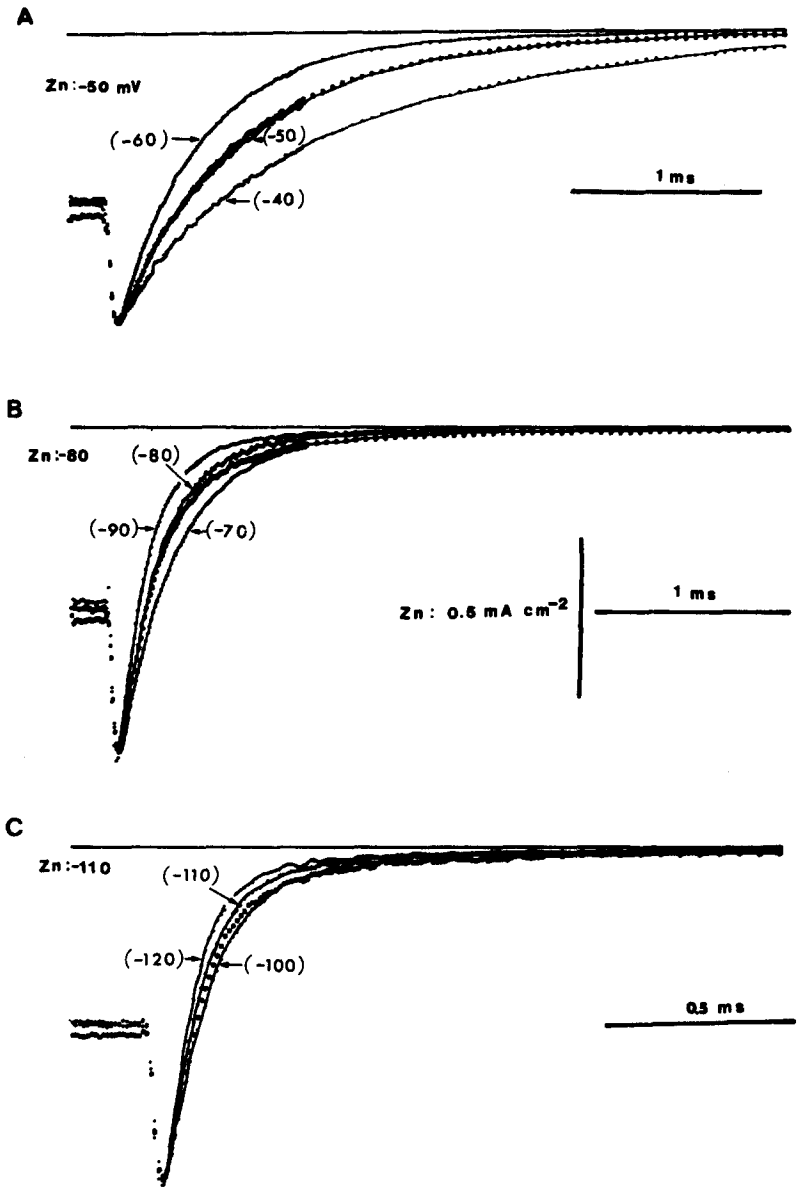

FIGURE 3. Superposition of I_{Na} OFF traces recorded in 116 Na ± 30 Zn^{2+} at different voltages after a 1-ms pulse to 0 mV. The figure is analogous to Fig. 2, but illustrates the rate of channel closing instead of opening. I_{Na} OFF in 30 Zn^{2+} was recorded at the indicated voltage; control currents were recorded as indicated in parentheses. Vertical I_{Na} scale bar applies to Zn^{2+} traces only; controls have been scaled to match the peak amplitude of the Zn^{2+} trace. In no case is the time course of I_{Na} OFF greatly altered by Zn^{2+}. Same axon as Fig. 2.

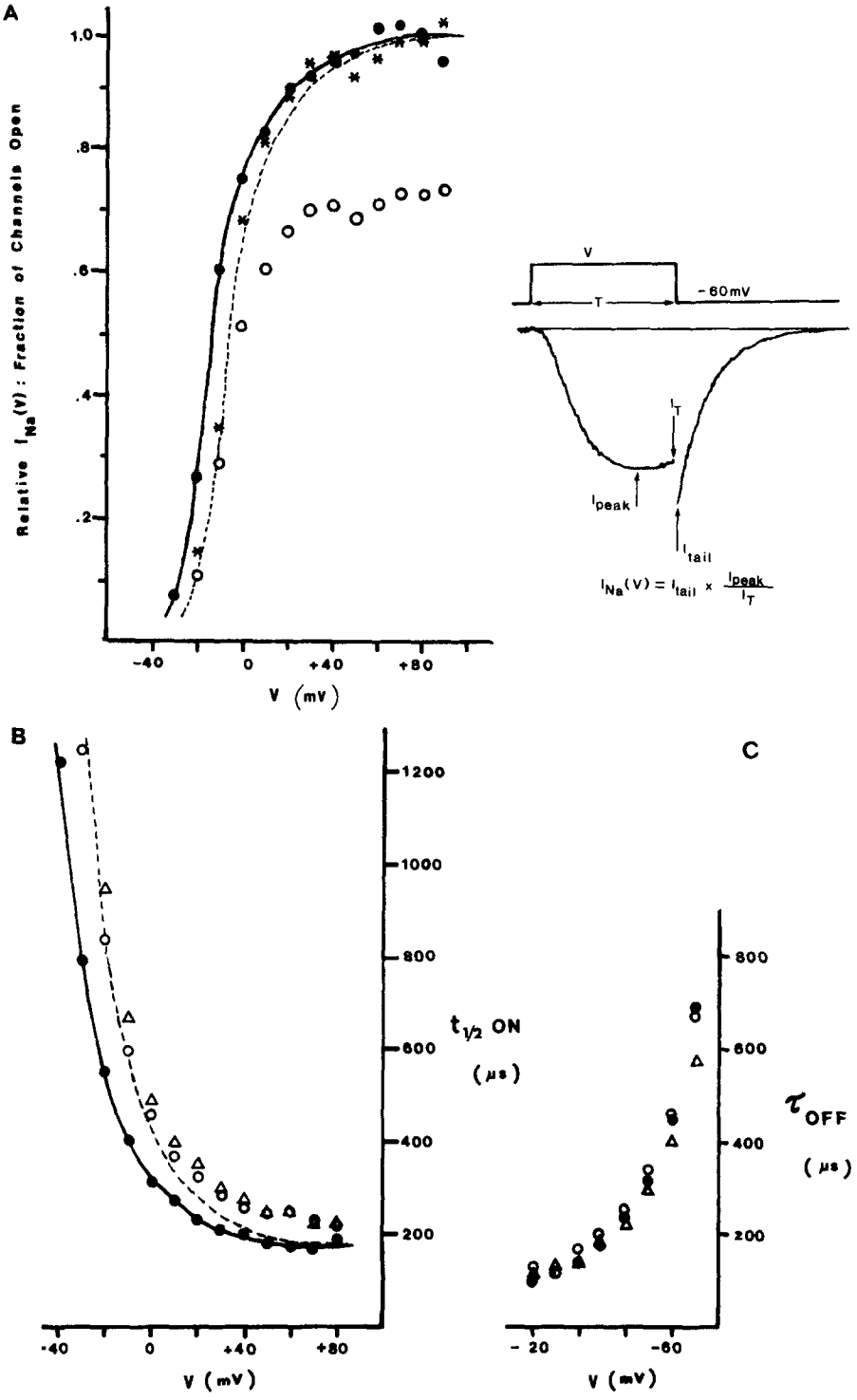
A
Relative $I_{Na}(V)$: Fraction of Channels Open
1.0
.8
.6
.4
.2
-40
0
+40
+80
V (mV)
V
T
-60mV
I_T
I_{peak}
I_{tail}
$I_{Na}(V) = I_{tail} \times \frac{I_{peak}}{I_T}$
B
1200
1000
800
600
400
200
$t_{1/2}$ ON
(μs)
-40
0
+40
+80
V (mV)
C
800
600
400
200
τ_{OFF}
(μs)
- 20
-60
V (mV)

measurements are made under the same driving force, and I_{Na} (V_f) is a measure of the maximum fraction of channels that open at each voltage.

Fig. 4A is a plot of the fraction of open channels vs. V without (closed dots) and with (open dots) Zn^{2+}. Asterisks represent the Zn^{2+} values multiplied by 1.33 to match the saturating value of 1.0 in the control solution. The number of channels opening at negative V is greatly decreased by Zn^{2+}, whereas at very positive V the effect is small. The dashed curve represents a +8-mV shift of the solid curve drawn by eye through the control points. It adequately fits the normalized Zn^{2+} data, which indicates a shift of the g_{Na}-V relation by this amount.

Zinc consistently reduced maximal g_{Na} (see Table I), but a detailed study of this effect was not carried out. Other divalent cations, including Ca^{2+}, appear to act similarly (Brismar, 1980; Arhem, 1980). The mechanism is not clear, but may involve a decrease in single-channel conductance (Conti et al., 1976).

Comparison of Zinc Effects on Opening and Closing Kinetics

In contrast to predictions based on surface charge theory, the g_{Na}-V shift is not equal to those for ON and OFF kinetics. Figs. 4B and C directly compare shifts of kinetics and of the g_{Na}-V curve. In each figure points are plotted for two runs in 30 mM Zn^{2+} (open symbols), which bracketed the control measurements. Half-time to peak current ($t_{1/2}$ ON) is the measure of ON kinetics. Fig. 4B shows that a +12-mV shift of the control $t_{1/2}$ ON-V relation (solid curve) fits the Zn^{2+} data (dashed curve) for small pulses, but not for large ones, where a much larger shift would be required (see also Fig. 2). Control and zincked $t_{1/2}$ ON-V curves may approach different asymptotes at very positive potentials,

FIGURE 4. (*opposite*) Comparison of Zn^{2+} effects on the equilibrium g_{Na}-V curve (A), and opening (B) and closing (C) kinetics. Same axon as Fig. 2. A. Fraction of Na channels open at the time of peak I_{Na} is plotted as a function of voltage, V, in 116 Na (●) and 116 Na + 30 Zn^{2+} (○). Asterisks indicate Zn^{2+} points multiplied by 1.33 to match saturating value of control data. Solid curve was drawn through the control points by eye and shifted +8 mV along the V axis to give the dashed curve that adequately fits the scaled Zn points. Inset shows the procedure for measuring the fraction of open Na channels as the adjusted amplitude of the Na tail current (I_{tail}) at −60 mV after a pulse to V mV (−20 mV in the inset). T was adjusted (1.2 ms in the inset) to return to −60 mV near the time of I_{peak}. I_T was usually within 10% of I_{peak}. The fraction of open channels at any voltage is proportional to I_{Na} (V) and is obtained as indicated. B. Half-time to reach peak I_{Na} ($t_{1/2}$ ON) as a function of voltage in 116 Na (●) and 116 Na + 30 Zn^{2+} (○, △ represent two runs bracketing control measurements). Solid curve was drawn by eye through control points and shifted +12 mV to give the dashed curve. The shifted curve fits the Zn^{2+} points for small pulses but not for large ones. C. Time constant of I_{Na} OFF vs. voltage in 116 Na (●) and 116 Na + 30 Zn^{2+} (○ and △ represent two runs as in B). Exponentials were fit using the computer to traces like those in Fig. 3 between the peak tail amplitude and a point ~10% of this amplitude from the baseline. No significant effect of Zn^{2+} is apparent.

but accurate measurement is difficult because of contamination by gating current.

OFF kinetics are plotted as the time constant of tail current decay (τ_{OFF} vs. V) in Fig. 4C. Both control and Zn^{2+} traces were generally well fit with a single exponential. Values of τ_{OFF} from two Zn^{2+} runs (open symbols) and one control run plotted against V indicate that there is no systematic effect of Zn^{2+} within experimental accuracy. In a few experiments, a slight shift (speeding) of OFF kinetics was observed (see Table I), but it was always far smaller than the shift in ON kinetics.

These three differential effects of Zn^{2+} were observed in every fiber studied: (*a*) a strong shift of ON kinetics, equivalent to +25–30 mV worth of membrane potential, (*b*) a smaller effect on the equilibrium level of open channels (less than a +10 mV shift in the g_{Na}-V relation), and (*c*) essentially unaffected OFF kinetics. Results from five fibers in which complete measurements were performed are summarized in Table I.

TABLE I

"SHIFTS" OF g_{Na} PARAMETERS BY 30 mM Zn^{2+}

Fiber	ON Kinetics	OFF Kinetics	g-V curve	g_{max} (Zn) / g_{max} (control)
	mV	*mV*	*mV*	*mV*
AU188C	+30 to +40	+2	+8	0.72
AU188D	+20 to +25	0	+5	0.75
JL288D	+30 to +40	+2	+13	0.83
SE058A	+30 to +40	—	+10	0.71
JN229B	+20	—	+6	0.83
Mean	+29.5	<+2	+8.4	0.77

Effect of 30 mM $ZnCl_2$ in the presence of 10 mM $CaCl_2$ on Na channel activation determined from I_{Na} measurements. "Shifts" of the apparent voltage dependence of opening (ON) kinetics were determined by superimposing traces recorded at different voltages (large depolarizations) in the presence and absence of Zn^{2+} (e.g., Fig. 2). Shifts of closing (OFF) kinetics were determined from plots of τ_{OFF} vs. V with and without Zn^{2+} (e.g., Fig. 4C). Shifts of g_{Na}-V relation were determined from similar plots (e.g., Fig. 4A). Mean values were obtained by averaging values for the individual fibers, or of the midpoint of the range indicated.

Zinc Does Not Enter and Plug Na Channels

Divalent cations also interact with Na channels in ways that are not thought to involve fixed surface charge. Woodhull (1973) postulated that external Ca ions and protons are drawn into Na channels at negative voltages and plug the conducting pore. Attraction to the pore grows with internal negativity, making the plugging voltage dependent. These ideas explain the Ca^{2+}-induced changes in the shape of the instantaneous I_{Na}-V relation in squid axon (Taylor et al., 1976). In the presence of high Ca^{2+}, many Na channels are blocked at negative voltages but conduct normally at positive voltages. Changes in closing (and possibly opening) kinetics caused by high Ca^{2+} (Frankenhaeuser and Hodgkin, 1957) may reflect this phenomenon to an unknown extent.

Zinc does not block Na channels in such an obviously voltage-dependent manner. Fig. 5A shows instantaneous I_{Na}-V curves obtained in the control solution (12 mM Ca^{2+}, filled circles) and after adding 30 mM Zn^{2+} (open circles). Current amplitude was measured at the plotted V after a brief activating pulse to +80 mV. At negative voltages I_{Na} is smaller in Zn^{2+}, but the I-V curve has approximately the same shape as the control. Nonlinearity in the control I-V curve probably results from plugging of Na channels by 12 mM Ca^{2+}, a nonlinearity that is not augmented by the addition of 30 mM Zn^{2+}. The triangles give the I_{Na}-V curve for the same axon in 50 mM Ca^{2+} (no

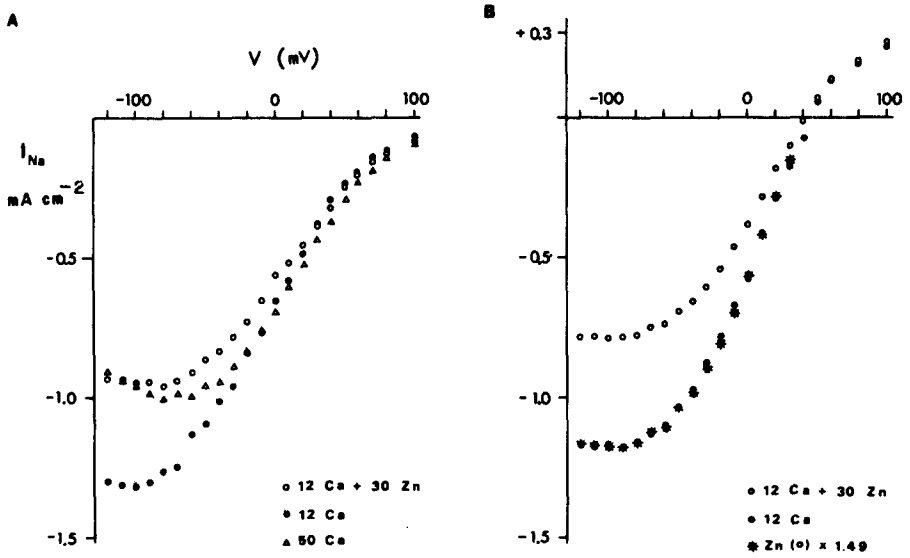

FIGURE 5. Zn^{2+} and the instantaneous I_{Na}-V relation in pronase-treated axons. A. Amplitude of I_{Na} measured at the indicated voltage 40 or 50 μs after the termination of a pulse to +80 mV. Measurements are plotted for 12 Ca^{2+} (●), 30 mM Zn^{2+} (○), and 50 mM Ca^{2+} (△). Zn^{2+} and Ca^{2+} show qualitatively different effects. Axon JL181G. B. I_{Na}-V curve for an axon with 20 mM internal Na. Current was measured after a 2-ms activating pulse to +50 mV. Inward current in 30 mM Zn^{2+} (○) matches controls (●) over the entire voltage range when scaled 1.49× (*), which indicates the reduction in g_{Na} caused by Zn^{2+} is not voltage dependent. Outward current is not reduced by Zn^{2+}. Axon JL021A.

Zn^{2+}). The additional 38 mM Ca^{2+} increases the nonlinearity of the curve and induces a negative resistance region. The qualitative difference between the 50 Ca^{2+} and 30 Zn^{2+} I-V curves indicates that Zn^{2+} does not act like Ca^{2+}.

Similar results from an axon that contained 20 mM Na in the internal perfusate are shown in Fig. 5B. The Zn^{2+}-induced reduction of inward I_{Na} is not voltage dependent, as shown by scaling the Zn^{2+} points by a factor of 1.49 (asterisks). The scaled Zn^{2+} curve almost perfectly matches the control curve from +30 to −120 mV. Thus, Zn^{2+} reduces inward I_{Na} by a voltage-independent mechanism.

Surprisingly, Zn^{2+} does not reduce outward I_{Na} in Fig. 5B, although it did slow the development of the outward I_{Na} tails (unpublished data). The mechanism by which Zn^{2+} reduces inward I_{Na} without changing outward current is unknown and deserves further investigation.

Zinc and Its Effect on Na Channel Gating Current (I_g)

Another signal generated during Na channel activation and deactivation is gating current, a capacitive charge movement reflecting operation of the channels' voltage sensors. If Zn^{2+} affects Na channels by interaction with the gating apparatus, gating current should be sensitive to Zn^{2+}. Because of an antagonism between Zn^{2+} and tetrodotoxin (TTX; see also below), we found it necessary to obtain I_g records in the absence of TTX. The possibility that residual ionic current through unpoisoned Na channels may complicate the observations to be subsequently described must be dealt with first.

Armstrong and Bezanilla (1974) showed that TTX does not markedly affect the time course or amplitude of I_g ON. We have more critically re-examined this question and confirm their conclusion. Examples of I_g ON before and during TTX application are shown in Fig. 6 for two different voltages. The no-TTX records are the ones of larger amplitude, and the change in gating current upon addition of TTX is obtained by subtraction (ΔI). Baselines to the ΔI traces were re-fitted to the points preceding the pulse.

At +40 mV no inward ΔI current can be seen. The TTX trace superimposes nearly perfectly on the control if scaled 1.10×. More serious contamination should exist at 0 mV, where the driving force is larger, and there is a small inward difference current that has the approximate time course of I_{Na} (see Fig. 2). From these records we conclude that contamination by ionic current is acceptably small.

Zinc Slows I_g ON, but Does Not Greatly Affect I_g OFF

Gating current transients during (I_g ON) and after (I_g OFF) a 0.5-ms pulse to +40 mV are shown in Fig. 7A. Charge carried across the membrane during the ON transient (Q_{ON} = 1,680 $e^-/\mu m^2$) approximately equals the OFF charge (Q_{OFF} = 1,970 $e^-/\mu m^2$). Q_{OFF} exceeds Q_{ON} probably because of a small Ca influx through Na channels (Meves and Vogel, 1973; Meves, 1975; Taylor et al., 1976).

This fiber (and all others for I_g data reported here) was not pronased, and the inactivation mechanism is thus operational. Pronase treatment itself does not alter the time course of I_g ON or of I_g OFF for a brief pulse (Armstrong and Bezanilla, 1977; Swenson et al., 1981), thus justifying comparison of our I_{Na} and I_g data (see below).

Zinc affects I_g in ways parallel to its action on I_{Na}. Superposition of I_g before (solid trace) and during (dotted trace) Zn^{2+} exposure in Fig. 7B shows that I_g ON is significantly slowed, whereas the time course of I_g OFF is little changed. Total charge transferred at this voltage is unaltered by Zn^{2+} (Q_{ON} = 1,670 $e^-/\mu m^2$), and approximate Q_{ON}:Q_{OFF} equality is maintained (Q_{OFF} = 1,990 $e^-/\mu m^2$).

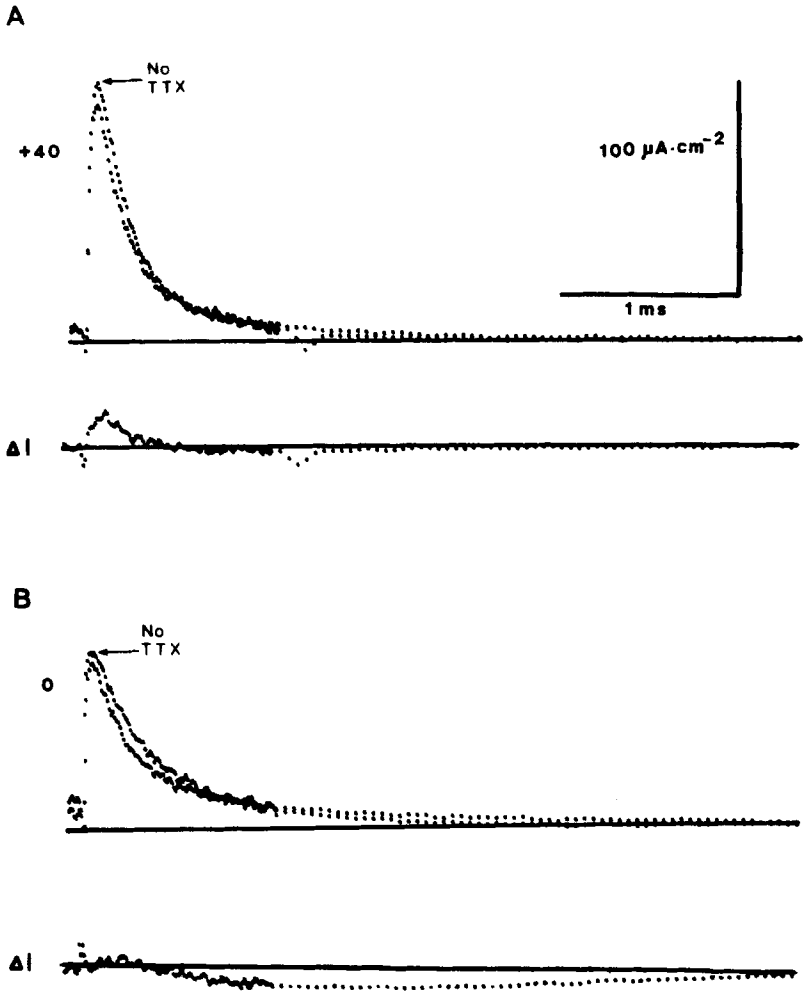

FIGURE 6. Effect of TTX on I_g ON at +40 mV (A) and 0 mV (B). At both voltages the pre-TTX trace is of larger amplitude. Subtraction of before and after TTX traces and refitting of baselines in the difference current to the points before the start of the pulse results in the ΔI trace below each pair. At +40 mV ΔI has the same time course as I_g itself; at 0 mV ΔI has a time course similar to that which I_{Na} would have (e.g., Fig. 2). Axon SE018G. Control pulses: P/4 from −180 mV.

Slowing of I_g ON by Zn^{2+} is more severe for large depolarizations, as was the case with I_{Na}. Fig. 7C shows I_g ON records with (dotted traces) and without Zn^{2+} over a large range of voltage. At +50 and +30 mV the peak of I_g is depressed and delayed, the subsequent decay is slowed, and total charge transfer is not much affected. For the smallest pulse illustrated, to −30 mV, the time course of I_g ON is not greatly changed, but the total charge transferred

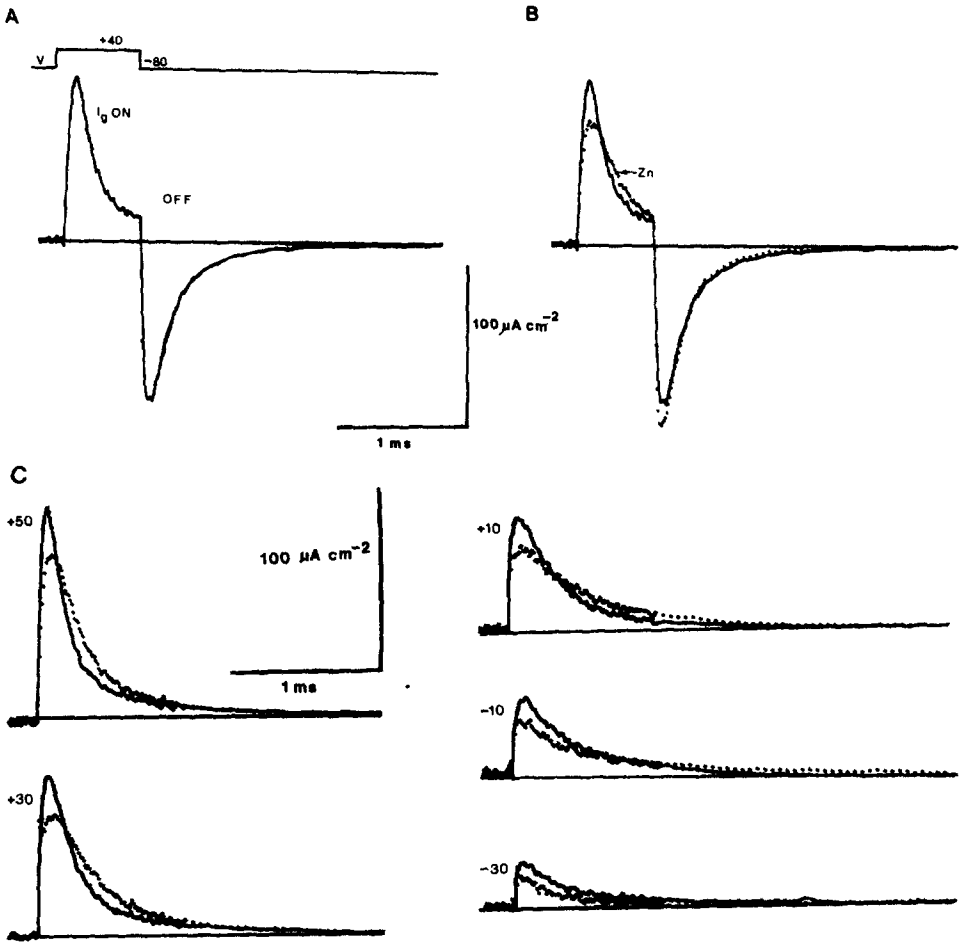

FIGURE 7. Effect of 30 mM Zn^{2+} on gating current (I_g). A. I_g ON during a 0.5-ms pulse from −80 mV to +40 mV and I_g OFF after return to −80 mV are illustrated. I_g was recorded in 0 Na (no TTX) using standard methods (see Methods, this paper, and also Armstrong and Gilly, 1979). Charge transferred in the ON transient approximately equals that in the OFF response. B. Effect of 30 mM Zn^{2+} on I_g recorded exactly as in A. Dotted Zn^{2+} trace has been plotted along with the solid control trace from A. The peak I_g ON is decreased in amplitude and prolonged; the subsequent decay of I_g ON is slowed. I_g OFF is little changed by Zn^{2+}; a slight acceleration is seen. Total charge transferred in ON and OFF responses is also unaffected by Zn^{2+}. C. I_g ON at a series of voltages as indicated in the absence (solid traces) and presence (dotted traces) of 30 mM Zn^{2+}. The slowing of I_g ON kinetics in Zn^{2+} seen with the large pulses (e.g., +30 and +50 mV) is not so apparent with small pulses (e.g., −30 mV). Charge transferred for the small pulses is much smaller in Zn^{2+} than in the control traces. Axon SE058B. Control pulses: P/4 from −130 mV.

is substantially reduced. For intermediate-sized pulses, the Zn effect is between the small and large pulse extremes.

The results in Fig. 7 show that Zn^{2+} apparently slows the gating reaction leading to Na channel opening, but the gating apparatus can still close the channel at the normal rate upon repolarization. In qualitative agreement with results on I_{Na}, Zn^{2+} produces a large effect on the kinetics of I_g ON and a much smaller effect on I_g OFF. For large pulses the number of operational channels, as judged by the total gating charge transferred is apparently not reduced by Zn^{2+}.

Quantifying the Zn^{2+} Effects on Gating Current

To quantitatively compare the action of Zn^{2+} on I_g and I_{Na}, the following approaches have been taken: (*a*) I_g ON kinetics are examined by superposition of records obtained with and without Zn^{2+} at different voltages; (*b*) a measurement of I_g OFF kinetics is obtained by fitting a single exponential to I_g OFF records after a strong, brief pulse; and (*c*) the total amount of gating charge transferred, measured by integration of I_g ON at various voltages, is used in determining the steady state *Q-V* distribution.

I_g ON KINETICS Fig. 8 illustrates I_g ON records before (solid traces) and during Zn^{2+} application in which direct comparison of ON kinetics is possible because approximately equal charge transfer occurred. At very positive voltages, Q_{max} is not much changed by Zn^{2+} (e.g., Figs. 7 and 10), and in Fig. 8A the +30-mV control matches both amplitude and time course of the Zn^{2+} trace at +60 mV fairly well. Thus, about +30 mV of additional depolarization are necessary to overcome the effect of Zn^{2+} at very positive voltages.

Zinc affects I_g ON kinetics for a small depolarization to a lesser extent. Q_{ON} for a small pulse is decreased by Zn^{2+} (e.g., Figs. 7 and 10), and in Fig. 8B the control −40-mV trace is indistinguishable from the −30-mV Zn^{2+} trace. This +10-mV shift of I_g ON kinetics due to Zn^{2+} for a small pulse compared with +30 mV for a large one agrees with the disproportionate effect of voltage on the slowing of I_{Na} kinetics by Zn^{2+}.

I_g OFF KINETICS Examples of exponential fits to I_g OFF at −80 mV in the presence and absence of Zn^{2+} are shown in Fig. 9A. The time constant is 230 μs in both cases. Fig. 9B is a plot of the time constant of I_g OFF vs. *V* with (open circles) and without Zn (closed symbols). The dashed curve reproduces the solid curve through the control points after shifting by +6 mV. Thus, Zn^{2+} causes a small speeding of the return of gating charge to its resting position. The effect is substantially smaller than the +30-mV shift of I_g ON kinetics, however. Direct comparison of these values for ON and OFF shifts is not so important as establishing the general idea that Zn^{2+} appears to affect the channel in a state-dependent way. More specifically, Zn^{2+} interacts more favorably with the channel in its closed state than in the open state, as indicated by a severely hindered opening rate in contrast with a minimally (if at all) promoted closing rate.

STEADY STATE Q-V DISTRIBUTION Q_{ON} with (open symbols) and without

Zn^{2+} is plotted vs. V in Fig. 10. At negative V, e.g., −50 to −20 mV, Zn^{2+} decreases Q_{ON}, but beyond 0 mV Q_{ON} is increased by ~10%. A small increase in total gating charge in Zn^{2+} was consistently seen, but is not completely understood. A similar increase in Q_{ON} was found when Ca^{2+} was increased from 10 to 50 mM (no Zn^{2+}). An increase in total Q with Ca^{2+} or Zn^{2+} was

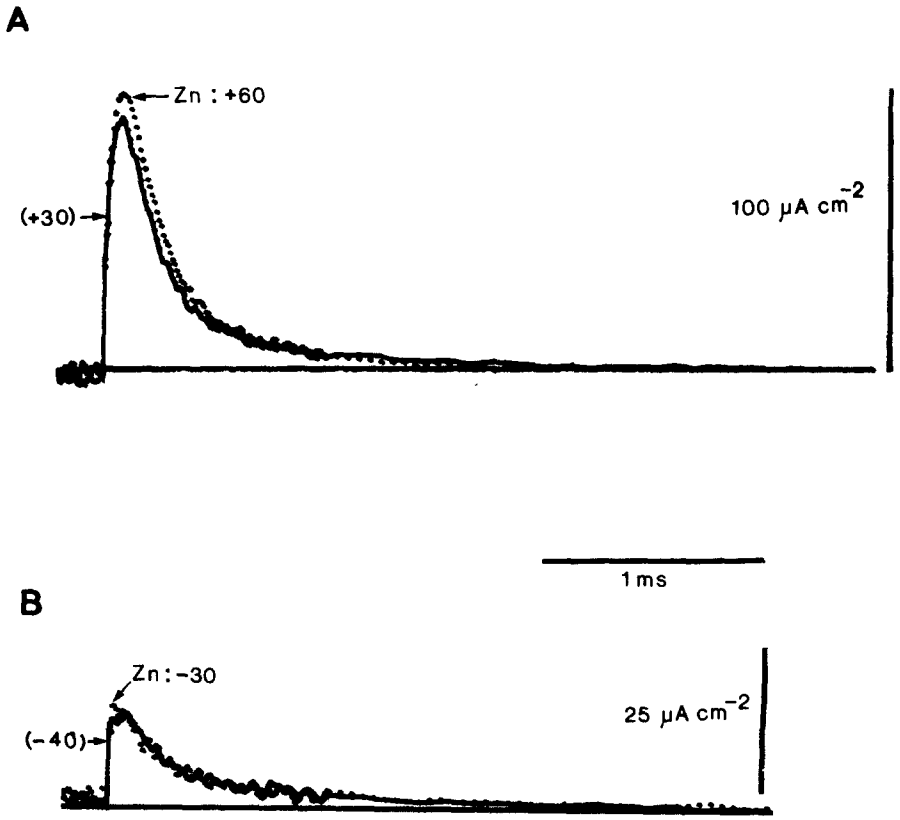

FIGURE 8. Effect of 30 mM Zn^{2+} on I_g ON kinetics for a large (A) and small (B) depolarization. I_g ON in 30 Zn^{2+} in both figures is the dotted trace recorded at the indicated voltage. Solid traces are control I_g ON records at the voltages indicated in parentheses. No scaling is involved in this comparison; I_g ON in 0 Na ± 30 Zn^{2+} at these particular voltages involves approximately equal charge transfer, allowing direct comparison of kinetics. As was the case with I_{Na} ON kinetics, the slowing of I_g ON by Zn^{2+} is more pronounced at more positive voltages. Same axon as Fig. 6.

also observed in the presence of TTX (unpublished data). A possible explanation is that increased divalent cation concentrations remove slow inactivation (Adelman and Palti, 1969), which may have been present at the holding potential (−80 mV), in the presence of our control 10-mM Ca^{2+} solution (Armstrong and Bezanilla, 1974; Meves, 1974; Meves and Vogel, 1977; Rudy, 1978).

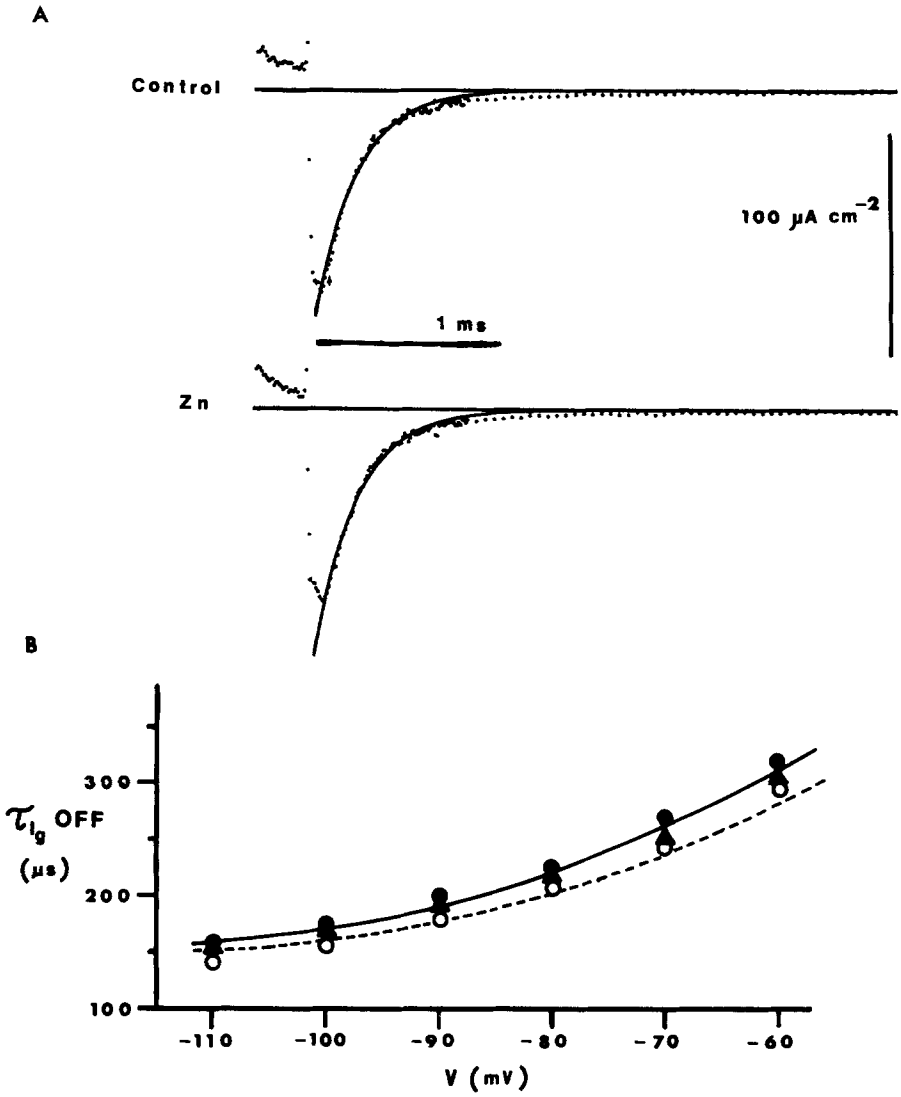

FIGURE 9. Effect of 30 mM Zn^{2+} on I_g OFF kinetics. A. I_g OFF traces at −80 mV after a 0.5-ms pulse to +50 mV. Control and Zn traces are illustrated with fitted exponentials superimposed. Fitting was from peak of I_g trace to about 10 points before change of sampling rate. A time constant of 230 μs fits both control and Zn^{2+} records. Axon AU318D. Control pulses: P/4 from −150 mV; holding potential = −90 mV. B. Time constant of I_g OFF decay obtained as in A at different voltages. (●) and (▲) are before and after Zn^{2+}; (○) represents 30 Zn^{2+}. Solid curve through control points has been shifted by +6 mV to give the dashed curve that fits the Zn^{2+} points reasonably well. Same axon as Fig. 6.

If the separation of the two Q-V curves in Fig. 10 is measured near the half-maximal point ($N = \sim 1{,}000\ e^-/\mu m^2$ at -20 mV), Zn^{2+} causes a shift of about +8 mV. Scaling the Zn^{2+} points 0.94× to match the saturating level of the control points increases the apparent shift to about +10 mV. These figures

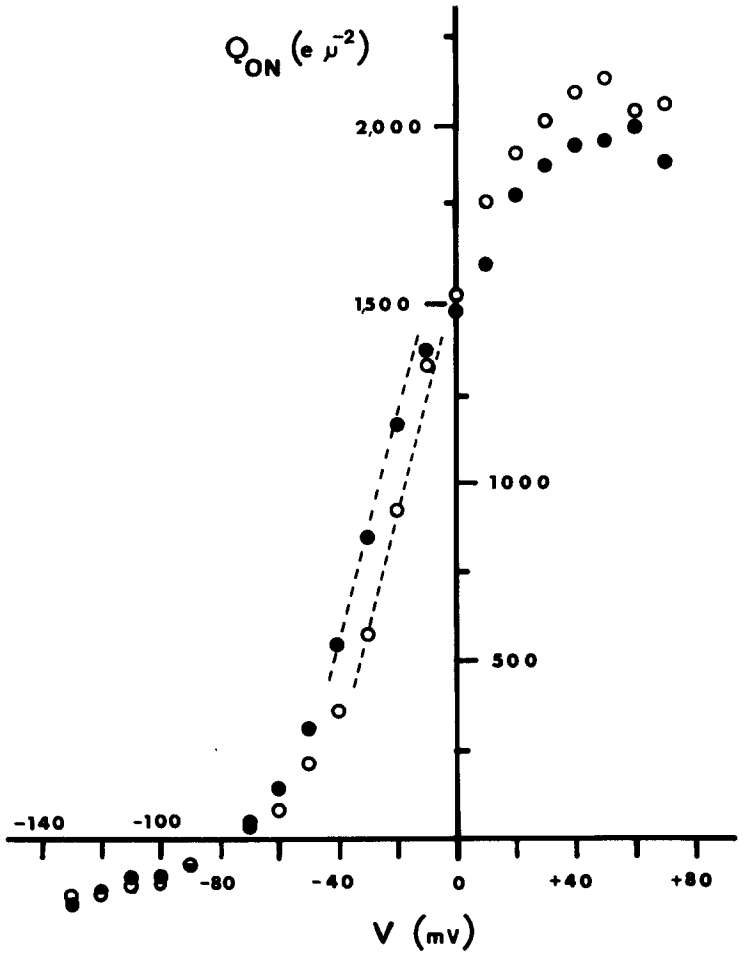

FIGURE 10. Zn^{2+} effect on the steady state Q-V relation. Q_{ON} values were obtained by integrating traces like those in Fig. 6C using the computer. Baselines were fit to final 1–2 ms of the records. (●) is the average of before and after Zn; (○) is in 30 Zn^{2+}. The effect on the Q-V curve can be approximately described as a shift of about +8 mV, the separation of the solid and dashed lines. Same axon as Fig. 6.

are substantially smaller than the maximal shift of +30 mV of I_g ON kinetics, and are again in qualitative agreement with results on g_{Na}.

For direct comparison with the g_{Na} results, the equivalent shifts of I_g parameters produced by 30 mM Zn^{2+} from the two most complete experiments

are indicated in Table II. Mean values from the g_{Na} results in Table I are also given. In each case, good agreement exists between the Zn^{2+} effect measured from I_{Na} and I_g records. ON kinetics are greatly affected by Zn^{2+}, the Q-V and g-V curves are affected less, and OFF kinetics are least affected. These results thus support the proposal that the primary effects of Zn^{2+} on g_{Na} are mediated by the interaction of Zn^{2+} with the gating apparatus.

Tetrodotoxin Interferes with the Action of Zinc

The effects on I_g produced by Zn^{2+} described above are not seen with TTX-poisoned fibers. Fig. 11 shows typical results from a Zn^{2+} experiment in the presence of 2×10^{-7} M TTX. I_g ON with (dotted traces) and without Zn^{2+} are shown at several voltages. Only for the largest pulse to +60 mV is a change with Zn^{2+} application evident, and this is qualitatively different from the

TABLE II

"SHIFTS" OF GATING CURRENT PARAMETERS BY 30 mM Zn^{2+}

Fiber	ON Kinetics	OFF Kinetics	Q-V curve	$\frac{Q_{max}\ (Zn)}{Q_{max}\ (control)}$
	mV	*mV*	*mV*	*mV*
AU318B	+20 to +30	0*	+4	1.06
SE058B	+30	+6	+8 to +10	1.12
I_g mean	+27.5	+6	+6.5	1.09
g_{Na} mean	+29.5	+2	+8.4‡	0.77

Effect of 30 mM $ZnCl_2$ in the presence of 10 mM $CaCl_2$ on Na channel activation determined from I_g measurements. "Shifts" of the apparent voltage dependence of opening (ON) kinetics were determined by superimposing traces recorded at different voltages (large depolarizations) in the presence and absence of Zn^{2+} (e.g., Fig. 8A). Shifts of OFF kinetics were determined from plots of τ_{OFF} vs. V with and without Zn^{2+} as described in Fig. 9B. Shifts of the Q-V relation were estimated near the midpoint of the curve as indicated in Fig. 10. Mean values were calculated as described in Table I.

* Measurement was made at −90 mV only (see Fig. 9A). Bottom row of entries contains the mean values from Table I for the effects of 30 mM Zn^{2+} on I_{Na}.

‡ Shift of g_{Na}-V curve.

change seen in the absence of TTX. Comparison of Figs. 7C and 11 suggests that when TTX is bound to the external mouth of the Na channel (Narahashi et al., 1967; Hille, 1975), it interferes with zinc's action on the gating apparatus. The antagonism between Zn^{2+} and TTX was not studied in detail.

DISCUSSION

Externally applied Zn ions slow ON kinetics of both I_{Na} and I_g as Na channels open, without much altering OFF kinetics. This cannot be explained as neutralization by Zn of a uniformly distributed layer of fixed surface charge. This surface charge theory predicts that both ON and OFF kinetic parameters must be equally shifted along the voltage axis, and that the effect of Zn^{2+} should be indistinguishable from a voltage change. Our results do not meet this prediction, nor can they be explained by postulating that Zn^{2+} serves as

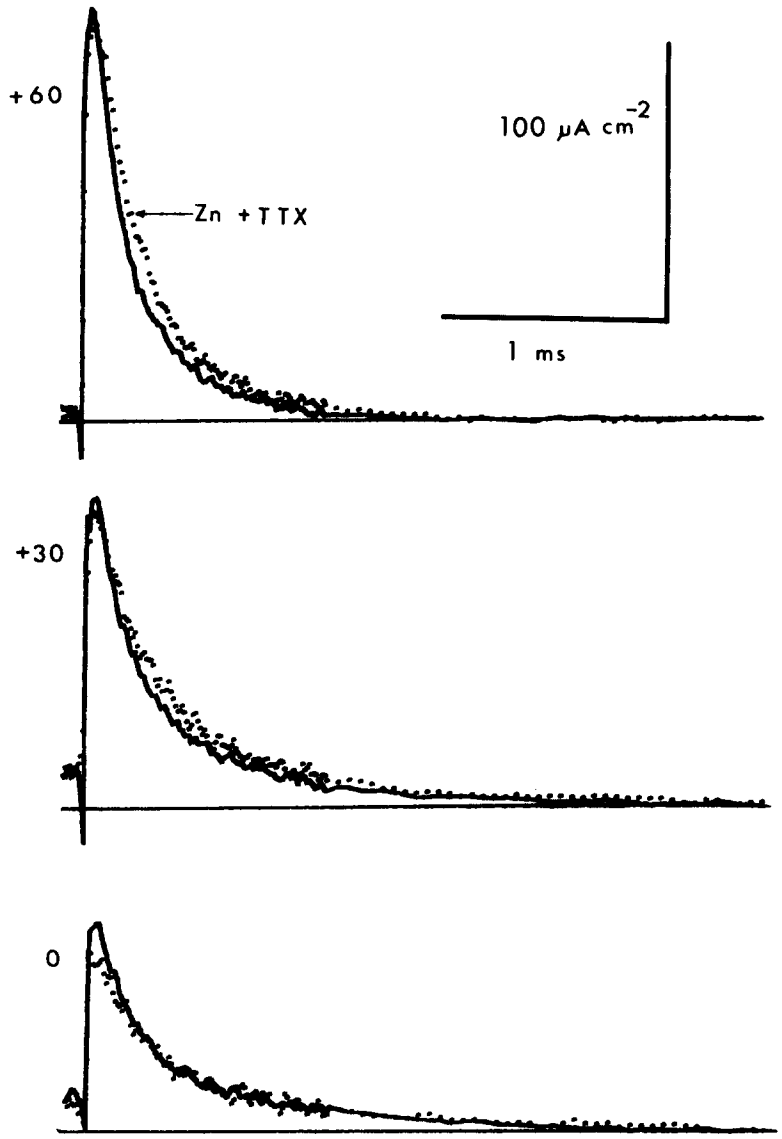

FIGURE 11. Effect of 30 mM Zn^{2+} on I_g ON in the presence of TTX. Control records in 0 Na + TTX (2×10^{-7} M) are the solid traces taken at the indicated voltages. Dotted traces are in 0 Na + TTX + 30 Zn^{2+}. Only at +60 mV is there any significant change in I_g produced by Zn^{2+}. TTX apparently protects the gating apparatus from Zn^{2+}. Axon SE018A. Control pulses: P/4 from −145 mV.

a voltage-dependent plug of Na channels. Instead, a more intimate interaction between Zn^{2+} and Na channel gating charge seems necessary.

One possibility, proposed by Tsien (1974) to account for the action of epinephrine on K channels in cardiac Purkinje fibers, is easily described in

terms of an energy barrier over which a charged, intramembranous gating particle must jump in order for the channel to undergo the transition between resting and activated states. Because the forward and backward rate constants of the reaction "depend upon opposite approaches to the energy barrier, they must in turn depend upon the electric field over different segments of the particle's path through the membrane." Shrager (1974) has made similar suggestions in regard to protons acting on K channels in crayfish axon.

We have incorporated their ideas into an explanation that also takes into account the following three considerations. (*a*) Opening and closing of Na channels involves movement of gating charges through the membrane electric field, manifested as gating current. (*b*) The hydrophobic interior of the membrane is hostile to free charge, making it likely that gating charge occupies stable positions only at the membrane surfaces. (*c*) Gating charge at a

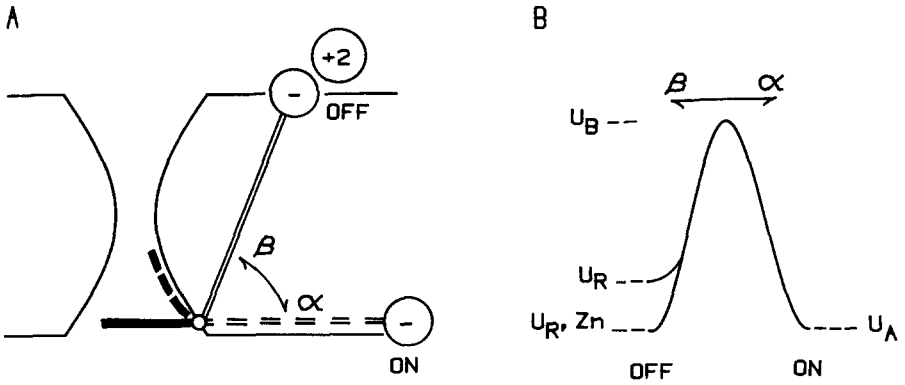

FIGURE 12. A simplified gating model and its energy diagram. The model accounts for the effect of Zn^{2+} as explained in the text.

membrane surface would polarize the adjacent aqueous medium, attracting cations or anions, depending on its charge.

Fig. 12 presents a simplified model satisfying these points. The gate pictured in Fig. 12A is controlled by a single negatively charged gating particle, with resting (OFF) position at the outer membrane surface and activated position at the inner surface. Movement of the charge on depolarization opens the gate and simultaneously produces an outward gating current. A positively charged particle moving in the opposite direction could equally well be imagined, but, as explained in the following paper on K channels (Gilly and Armstrong, 1982), this is not compatible with the effects of Zn^{2+} and Hg^{2+}.

Fig. 12B is an energy diagram for the opening reaction (Glasstone et al., 1941), relating the potential energies of the resting (U_R) and the activated (U_A) states to the forward and backward rate constants of the reaction, α and β. U_B-U_R and U_B-U_A are the respective energies of the opening and closing

transitions, and are related to α and β by the equations:

$$\alpha = Ce^{-\left(\frac{U_B - U_R}{kT}\right)}$$

$$\beta = Ce^{-\left(\frac{U_B - U_A}{kT}\right)}.$$

C is a constant that determines the absolute reaction rate.

In its resting position the gating charge polarizes the external medium, attracting divalent cations more strongly than monovalents (Fig. 12A). Electrostatic attraction between gating charge and counterion would stabilize the gating charge at its resting position. In the energy diagram, stabilization is indicated as a lowering of the energy $U_R(U_R, Zn)$. This increases the energy barrier for the resting → activated transition and decreases α.

With sufficient depolarization, the gating charge jumps to the inner membrane surface (Fig. 12A) and the previously enriched counterions quickly diffuse away from the membrane, making the solution adjacent to the charge's OFF position electrically neutral. Thus, the presence of divalent cations in the external solution does not affect the gating particle in the activated position and leaves β unchanged.

This simple gating model explains in principle how Zn^{2+} can slow I_{Na} and I_g ON kinetics without altering OFF rates. With a decreased α and unchanged β, the equilibrium number of open channels in a population [proportional to $\alpha/(\alpha + \beta)$ in the simple model] would also be smaller than normal at any voltage where β was not negligibly small. These are the three effects of Zn^{2+} that we have described in detail in the Results.

Modeling the Zinc Effect on Na Channel Activation

The principles just discussed can be readily incorporated into a gating model that accurately predicts g_{Na}, I_g, and the Zn^{2+} effect. The kinetic scheme used was (see also Armstrong and Gilly, 1979):

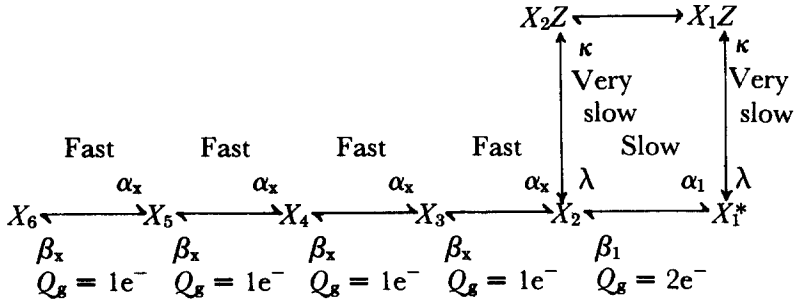

In this scheme, X_6 through X_2 are closed states; X_1^* is the only conducting state, and X_1Z and X_2Z are inactivated states. The first four steps are fast and involve gating charge movement (Q_g) equivalent to the transfer of one electronic charge all the way across the membrane. The final step is slow and is accompanied by the apparent transfer of two electronic charges. That the rate-limiting last step is more voltage sensitive than the early steps (i.e.,

involves more gating charge movement) has now been verified experimentally (Gilly et al., 1981).

Some of the steps may involve disappearance of a negative charge from the membrane's outer surface on activation, as in the simple model described above. These steps would be expected to be sensitive to Zn ions in the external medium. To ascertain how many such steps there might be, we have tested three variations of the kinetic model above and found that two of them give a reasonable fit to the Zn^{2+} data. The three cases were:

Model I: zinc only interacts with gating charges when the channel is in the fully closed (resting) state by creating a special state, X_{Zn}, to the left of X_6. Zinc thus temporarily paralyzes the entire channel at the onset of activation but does not alter any of the subsequent rate constants in the sequence. The reaction would therefore be formally slightly different than the simple model discussed above and can be represented (see also Armstrong and Gilly, 1979):

$$X_{Zn} \underset{\beta_{Zn}}{\overset{\alpha_{Zn}}{\rightleftarrows}} X_6 \rightleftarrows X_5 \rightleftarrows X_4 \cdots$$

Model II: according to the principles discussed in conjunction with the simple gating model, zinc interacts with each gating charge and slows all forward rate constants in the six-state activation sequence equally but does not alter any reverse rate constants. Thus, α's in Zn^{2+} are smaller than the control α values by a constant fraction at all voltages.

Model III: zinc selectively slows the first ($X_6 \rightharpoonup X_5$) and last ($X_2 \rightharpoonup X_1^*$) steps only, but again does not alter the backward rate constants, or any of the other forward rate constants.

Sample calculations for the control case and for the three Zn models (see also below) are shown in Fig. 13, and parameters of the fits are listed in Table III. Experimental I_{Na} and I_g records at several voltages are illustrated along with the corresponding calculations. The uppermost set of traces in Fig. 13A shows control data records (averages of before and after Zn^{2+}) at +10 mV along with the calculated traces (solid curves). Control records and their fits at other voltages are given as the upper set of traces in Figs. 13B–D, and voltage is indicated in each case. As can be seen, the fits are acceptable, and the model thus predicts the correct time course and amplitude of both I_{Na} and I_g over the full range of activation in the absence of Zn^{2+}.

As indicated in Table III, there are several significant constraints to the control fitting. (*a*) Ratios of forward to backward rate constants (i.e., equilibrium constants) were predicted according to a Boltzman distribution as described in the legend. (*b*) The calculated conductance was scaled by the correct driving force for each voltage. (*c*) The rate of inactivation (given by κ and λ) was nearly independent of voltage. The final slow phase of I_g at +50 mV is not accounted for by this model. Part of this slow charge movement may be related to K channel activation, and the remainder is unexplained (Gilly and Armstrong, 1980*c*).

Calculations for the Zn^{2+} effect at +10 mV using model I are shown in Fig. 13A directly below the control traces. Although good fits can be obtained to

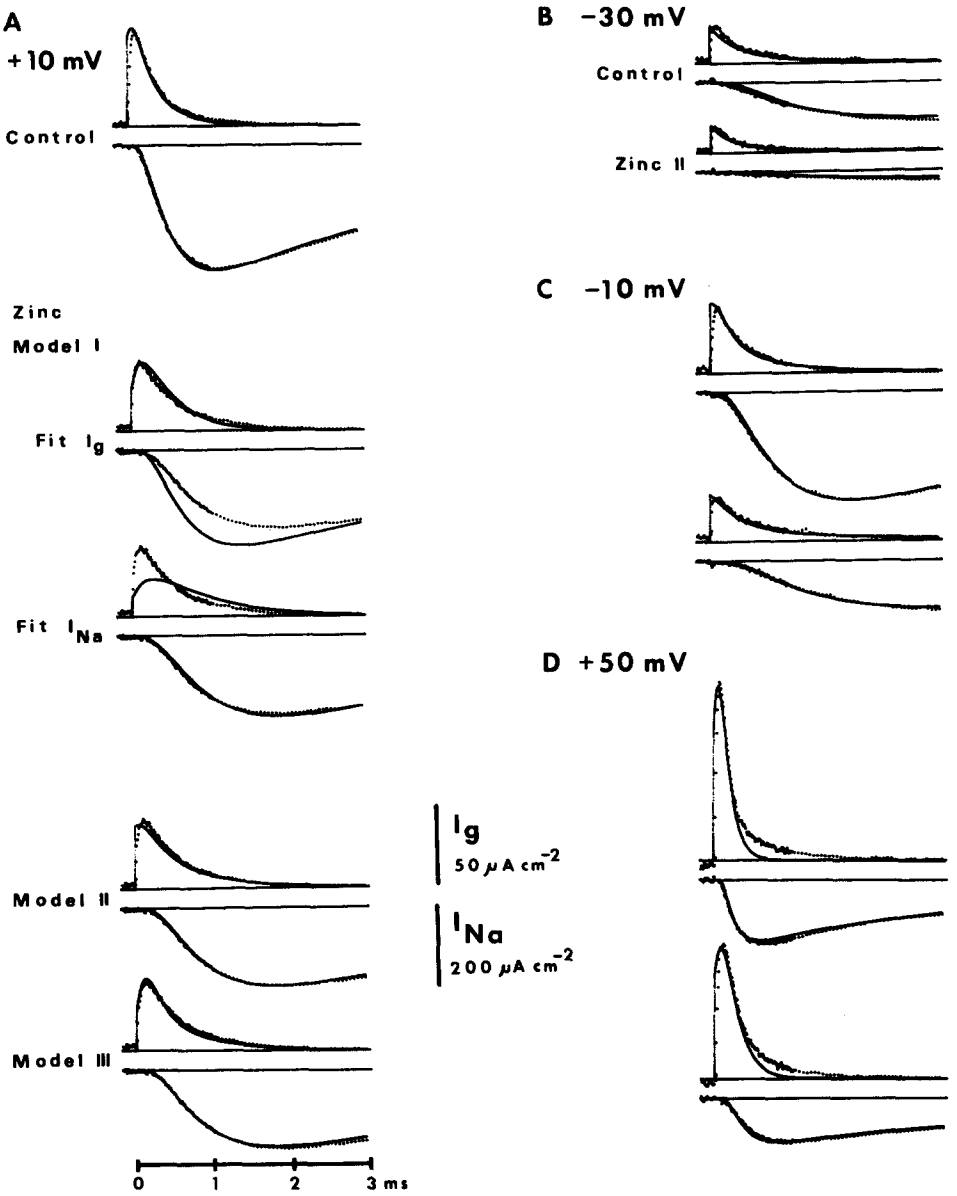

FIGURE 13. Calculations based on the model described in the text and more completely in Armstrong and Gilly (1979) for control I_{Na} and I_g ON and for zincked I_{Na} and I_g ON with Zn models I, II, and III. In each pair of superimposed traces, the solid trace is the calculation and the dotted one is the experimental record. I_{Na} data from the same axon as in Fig. 6; I_g data from SE058A of the same squid. A. Control and Zn I–III traces and calculated fits at +10 mV. Two cases for model I are shown. Either I_g or I_{Na} can be fit, but not both simultaneously. Models II and III both give good fits to both I_{Na} and I_g. B–D. Control and Zn model II fits at −30, −10, and +50 mV, as indicated. See text and Table III for details.

TABLE III

Control model	α_1	α_x	β_1	β_x	κ	λ	Initial conditions
+50 mV (Fig. 13D)	9	30	0.016	1.25	0.3	0.05	$X_6 = 1.0$
+10 mV (Fig. 13A)	3.8	20	0.16	4.12	0.3	0.05	$X_6 = 1.0$
−10 mV (Fig. 13C)	1.9	15.5	0.40	7.11	0.3	0.05	$X_6 = 1.0$
−30 mV (Fig. 13B)	1.2	8.5	1.22	8.67	0.24	0.05	$X_6 = 1.0$
+40 mV ON (Fig. 14)	6	27	0.023	1.68	0.3	0.05	$X_6 = 1.0$
−80 mV OFF (Fig. 14)	0.09	5.3	3.55	40	0.25	0.05	See legend

Zinc: Model I	α_{Zn}	β_{Zn}	κ	λ	Initial conditions
+10 mV (Fig. 13A)					
Fit I_g	30	40	0.25	0.05	$X_{Zn} = 0.57$ $X_6 = 0.43$
Fit I_{Na}	5	20	0.3	0.05	$X_{Zn} = 0.8$ $X_6 = 0.2$

Zinc: Model II	Reduction in α_1 and α_x ($\alpha_{Zn}/\alpha_{control}$)	κ	λ	Initial conditions
+50 mV (Fig. 13D)	0.70	0.25	0.05	$X_6 = 1.0$
+10 mV (Fig. 13A)	0.63	0.27	0.05	$X_6 = 1.0$
−10 mV (Fig. 13C)	0.63	0.30	0.05	$X_6 = 1.0$
−30 mV (Fig. 13B)	0.66	0.24	0.05	$X_6 = 1.0$
+40 mV ON (Fig. 14)	0.675	0.3	0.05	$X_6 = 1.0$
−80 mV OFF (Fig. 14)	0.64	0.25	0.05	See legend

Zinc: Model III	Reduction in α_x for first step and α_1 for last step ($\alpha_{Zn}/\alpha_{control}$)	κ	λ	Initial conditions
+10 mV (Fig. 13A)	0.447	0.25	0.05	$X_6 = 1.0$

Parameters used in calculating I_g and I_{Na} traces with control and zinc models I, II, and III. All rate constants are given in ms^{-1}. References to appropriate figures are given in parentheses. α and β were assumed to hold to the relations:

$$\frac{\alpha_x}{\beta_x} = \exp\left[\frac{Q_x(V - \bar{V}_x)}{25 \text{ meV}}\right] \quad \text{and} \quad \frac{\alpha_1}{\beta_1} = \exp\left[\frac{Q_1(V - \bar{V}_1)}{25 \text{ meV}}\right],$$

where $Q_x = 1$ and $Q_1 = 2$ electronic charges, respectively, and $\bar{V}_x = \bar{V}_1 = -29.5$ mV. To fit currents after zincking the fiber, α_x and α_1 were reduced as indicated in table for models II and III; β_x and β_1 were unchanged. This corresponds to $\bar{V}_x$ and $\bar{V}_1$ values, respectively, of −18 to −20.5 mV and −23.7 to −24.7 mV for model II, and −10.5 and −19.4 mV for model III. I_{Na} at every voltage was scaled relative to that calculated at +50 mV by the appropriate difference in driving force, $(V_{Na} - V)/(V_{Na} - 50)$; V_{Na} was estimated to be +75 mV by extrapolation of the I_{Na}-V curve at very positive voltages. All I_{Na} traces in Zn^{2+} were calculated with the same scaling factor as for controls, but reduced by a constant factor of 0.75 at all voltages. The scaling factor for I_g was kept constant for I_g ON at all voltages, both in controls and Zn^{2+}, but the factor was increased by 1.10 for Zn^{2+}. I_g OFF scaling factor for controls and Zn^{2+} was increased by 1.18 to match the ON:OFF inequality discussed in the text. Initial conditions for I_g OFF were taken as those existing at the end of the I_g ON calculation:

	X_1^*	X_2	X_3	X_4	X_5	X_6	X_{1z}	X_{2z}
Control	0.7926	0.0835	0.007	0.0007	0.0001	0	0.1065	0.0096
Zinc	0.6131	0.2446	0.0375	0.0091	0.003	0.001	0.0697	0.216

either I_{Na} or I_g separately, both waveforms cannot be acceptably fit with a single choice of α_{Zn} and β_{Zn}. At more negative voltages the result of attempting to fit both I_{Na} and I_g simultaneously is even worse (not illustrated); at +50 mV (not illustrated) the fits are only slightly better than at +10 mV. Clearly model I is inadequate. Similarly, slowing only the last step (or any other single step) is also insufficient to model the Zn^{2+} effects on both I_g and I_{Na} (not illustrated).

Fits with models II and III at +10 mV are shown as the bottom sets of traces in Fig. 13A. In model II, Zn^{2+} slowed every forward rate constant by a factor of 0.63. For model III, α's for the $X_6 \rightarrow X_5$ and the $X_2 \rightarrow X_1^*$ transitions only were both slowed by a factor of 0.45. Both models give very good fits to I_{Na} and I_g.

With the same Zn^{2+}-induced reduction of α values, models II and III give good fits over the full voltage range of activation. Figs. 13B–D presents control fits and model II fits at −30, −10, and +50 mV. The reduction of forward rate constants by Zn^{2+} amounted to a factor of 0.63–0.7 over this large voltage range. Model III (not illustrated) also gave acceptable fits over the entire voltage range with the reduction in α for the first and last steps being essentially independent of voltage.

Fig. 14 shows that model II adequately fits both I_g ON (+40 mV) and I_g OFF (−80 mV) if all α's are reduced by ~0.65× by Zn^{2+}. In agreement with observation (see also Fig. 6B), the model predicts that I_g OFF in Zn^{2+} is slightly larger in amplitude and faster than the control. This is not caused by an effect of the altered α values of the actual activated to resting transitions of the gating charges, but reflects the difference in the distribution of channels among the states at the end of the brief activating pulse (see the legend to Table III). Because I_g ON is slower in Zn^{2+}, more channels are still in closed states at pulse end. Rapid return of these channels to the X_6 state upon repolarization is responsible for the acceleration of I_g OFF predicted and observed in Zn^{2+}.

We do not find a speeding of I_{Na} OFF tails, however, nor does the model predict such an effect. Both experimental (see Fig. 3) and calculated (bottom pair of traces in Fig. 14, g_{Na}: with and without Zn^{2+}) kinetics for I_g OFF are unaltered by Zn^{2+}.

Modification of the control model to predict the effects of Zn^{2+} on both I_{Na} and I_g over the full range of activation is thus very simple, and we feel that two important conclusions can be drawn from these calculations. At least two charge movement steps must be independently slowed by Zn^{2+}. Moreover, the interaction of a Zn ion and gating charge is, strictly speaking, not voltage dependent but state dependent—the same reduction in α caused by stabilization of the closed state of the channel fits the opening kinetics at any activating voltage. This means that the Zn ion does not see an appreciable fraction of the membrane electric field.

Do Other Divalent Cations Act Like Zinc?

The relevance of our findings on Zn to other polyvalent cations remains to be established and is an important question. To our knowledge, Ca is the only

divalent cation for which Na channel ON and OFF kinetics have been previously reported. Calcium slows I_{Na} ON kinetics, but as discussed earlier it also enters and blocks Na channels, making analysis of I_{Na} OFF difficult. High Ca apparently does, however, slow I_g ON without much altering I_g OFF (Moore,

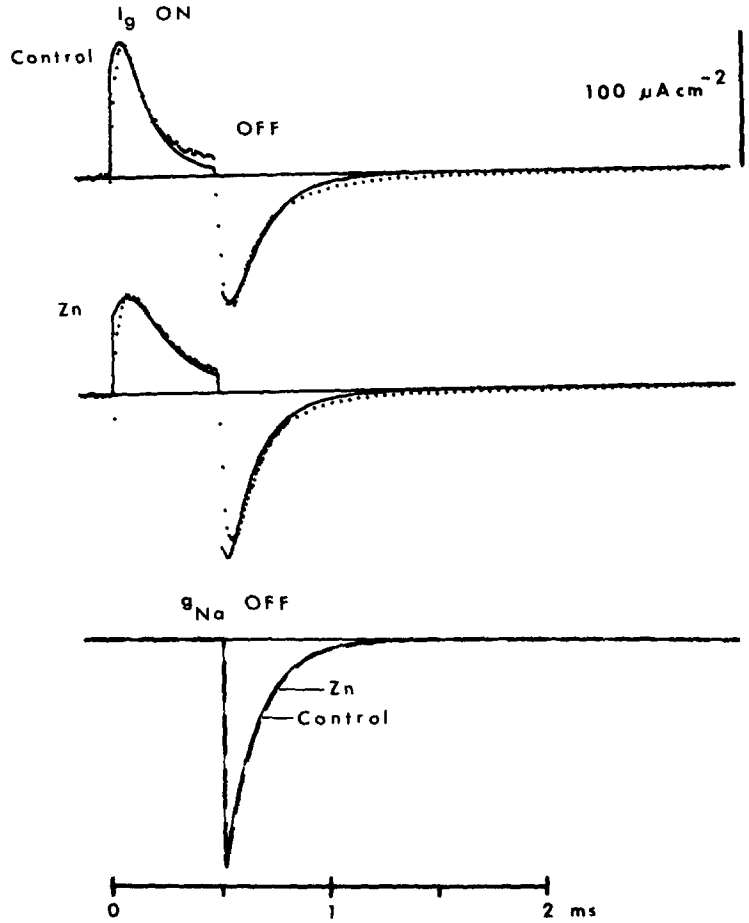

FIGURE 14. Observed and predicted currents with and without Zn^{2+}. Model II was used for calculation. Zincked I_g ON and OFF are both fitted fairly well with the same Zn^{2+}-induced reduction of forward rate constants. The slight acceleration of I_g OFF in Zn^{2+} seen experimentally is also predicted by the model. See text for explanation. The time course of g_{Na} OFF calculated with the same parameters as for the I_g traces is not altered by Zn^{2+} as shown by the bottom pair of traces. (Only calculated g_{Na} traces are illustrated.) See Table III for computational details. Same axon as in Fig. 13.

1978; Moore et al., 1977), which suggests that Ca may affect Na channel gating in basically the same manner as Zn does.

Results presented in this paper show that Zn ions do not affect Na channel gating via a bias voltage caused by neutralization of a sheet of fixed surface

charge. In the case of Zn, it is more realistic to consider a quite specific interaction of a divalent cation and the voltage sensor/gating apparatus of the Na channel. The interaction we propose is an electrostatic stabilization of exposed negative gating charges at the external membrane surface when the channel is closed.

Alternative proposals involving more complicated surface charge schemes cannot be entirely dismissed, however. For example, Zn^{2+} might be bound, not by a uniform sheet of fixed charge, but by a special charge close to the Na channel gating apparatus. Such binding of one or several Zn ions would result in a nonlinear electric field within the membrane interior, but unless the opening and closing gating reactions took place in different regions of the membrane, the Zn^{2+} effect should still be indistinguishable from a membrane voltage change. The model we present provides a mechanism for moving the gating particles around in the membrane where different Zn^{2+}-induced fields might exist. Although we cannot say with certainty whether Zn^{2+} is bound near the Na channel or is free in solution, we regard this for the present as academic. In the next paper we discuss more fully the implications of this question. Although fixed surface charges undoubtedly exist in nerve (see Introduction), it is clearly not necessary to postulate a significant role of such charges in mediating the action of extracellular Zn ions on Na channel gating.

Received for publication 1 September 1981 and in revised form 1 March 1982.

REFERENCES

ADELMAN, W. J., and Y. PALTI. 1969. The effects of external potassium and long duration voltage conditioning on the amplitude of sodium currents in the giant axon of the squid, *Loligo pealei*. *J. Gen. Physiol.* **54**:589–606.

ARHEM, P. 1980. Effects of some heavy metal ions on the ionic currents of myelinated fibres from *Xenopus laevis*. *J. Physiol. (Lond.)*. **306**:219–231.

ARMSTRONG, C. M., and F. BEZANILLA. 1974. Charge movement associated with the opening and closing of the activation gates of the Na channels. *J. Gen. Physiol.* **63**:533–552.

ARMSTRONG, C. M., and F. BEZANILLA. 1975. Currents associated with the ionic gating structures in nerve membrane. *Ann. N. Y. Acad. Sci.* **264**:265–277.

ARMSTRONG, C. M., and F. BEZANILLA. 1977. Inactivation of the sodium channel. II. Gating current experiments. *J. Gen. Physiol.* **70**:567–590.

ARMSTRONG, C. M., F. BEZANILLA, and E. ROJAS. 1973. Destruction of sodium conductance inactivation in squid giant axons perfused with pronase. *J. Gen. Physiol.* **62**:375–391.

ARMSTRONG, C. M., and W. F. GILLY. 1979. Fast and slow steps in the activation of sodium channels. *J. Gen. Physiol.* **74**:691–711.

BRISMAR, T. 1980. The effect of divalent and trivalent cations on the sodium permeability of myelinated nerve fibres of *Xenopus laevis*. *Acta Physiol. Scand.* **108**:23–29.

BROWN, R. H., JR. 1974. Membrane surface charge: discrete and uniform modelling. *Prog. Biophys. Mol. Biol.* **28**:341–370.

CHANDLER, W. K., A. L. HODGKIN, and H. MEVES. 1965. The effect of changing the internal

solution on sodium inactivation and related phenomena in giant axons. *J. Physiol. (Lond.)*. **180**:821–836.

COLE, K. S. 1969. Zeta potential and discrete vs. uniform surface charges. *Biophys. J.* **9**:465–469.

CONTI, F., B. HILLE, B. NEUMCKE, W. NONNER, and R. STÄMPFLI. 1976. Measurement of conductance of the sodium channel from current fluctuations at the node of Ranvier. *J. Physiol. (Lond.)*. **262**:699–727.

D'ARRIGO, J. S. 1978. Screening of membrane surface charge by divalent cations: an atomic representation. *Am. J. Physiol.* **235**:C109–C117.

DODGE, F. A. 1961. Ionic permeability changes underlying nerve excitation. *In* Biophysics of Physiological and Pharmacological Actions. A. M. Shanes, editor. American Association for the Advancement of Science. Washington, D. C. 119.

FRANKENHAEUSER, B., and A. L. HODGKIN. 1957. The action of calcium on the electrical properties of squid axons. *J. Physiol. (Lond.)*. **137**:218–244.

GILBERT, D. L., and G. EHRENSTEIN. 1969. Effect of divalent cations on potassium conductance of squid axons: determination of surface charge. *Biophys. J.* **9**:447–463.

GILLY, W. F., and C. M. ARMSTRONG. 1980*a*. Interaction of zinc ion and the sodium channel gating apparatus of squid axon. *Proc. Intl. Union Physiol. Sci.* **14**:433.

GILLY, W. F., and C. M. ARMSTRONG. 1980*b*. Interaction of external transition metal ions and the mobile gating charges of Na and K channels in squid axon. *Biol. Bull.* **159**:483.

GILLY, W. F., and C. M. ARMSTRONG. 1980*c*. Gating current and potassium channels in the squid giant axon. *Biophys. J.* **29**:485–492.

GILLY, W. F., and C. M. ARMSTRONG. 1981. Divalent cations, mobile gating charge and fixed surface charge in squid axon. *Biophys. J.* **33**:280*a*.

GILLY, W. F., and C. M. ARMSTRONG. 1982. Divalent cations and the activation kinetics of potassium channels in squid giant axons. *J. Gen. Physiol.* **79**:965–996.

GILLY, W. F., R. P. SWENSON, and C. M. ARMSTRONG. 1981. Sodium channel activation in pronased squid axons: the slow last step. *Proc. VII Int. Biophys. Congress*. Mexico City. 330.

GLASSTONE, S., K. J. LAIDLER, and H. EYRING. 1941. The Theory of Rate Processes. The Kinetics of Chemical Reactions, Viscosity, Diffusion and Electrochemical Phenomena. McGraw-Hill, Inc., New York. 1–50.

HILLE, B. 1968. Charges and potentials at the nerve surface. Divalent ions and pH. *J. Gen. Physiol.* **51**:221–236.

HILLE, B. 1975. The receptor for tetrodotoxin and saxitoxin. A structural hypothesis. *Biophys. J.* **15**:615–619.

HILLE, B., A. WOODHULL, and B. I. SHAPIRO. 1975. Negative surface charge near sodium channels of nerve: divalent ions, monovalent ions and pH. *Phil. Trans. R. Soc. Lond. B Biol. Sci.* **270**:301–318.

MCLAUGHLIN, S. G. A., G. SZABO, and G. EISENMAN. 1971. Divalent ions and the surface potential of charged phospholipid membranes. *J. Gen. Physiol.* **58**:667–687.

MEVES, H. 1974. The effect of holding potential on the asymmetry currents in squid giant axons. *J. Physiol. (Lond.)*. **254**:787–801.

MEVES, H. 1975. Calcium currents in squid giant axon. *Phil. Trans. R. Soc. Lond. B. Biol. Sci.* **270**:377–387.

MEVES, H., and W. VOGEL. 1973. Calcium inward currents in internally perfused giant axons. *J. Physiol. (Lond.)*. **235**:225–265.

MEVES, H., and W. VOGEL. 1977. Inactivation of the asymmetrical displacement current in giant axons of *Loligo forbesi*. *J. Physiol. (Lond.)*. **267**:377–393.

MOORE, J. W. 1978. On sodium conductance gates in nerve membranes. *In* Physiology and Pathobiology of Axons. S. G. Waxman, editor. Raven Press, New York. 145–153.

MOORE, J. W., M. WESTERFIELD, and S. JASLOVE. 1977. Calcium affects kinetics of sodium onset gates, but not reset gates. *Biophys. J.* **17**:14*a*.

NARAHASI, T., N. C. ANDERSON, and J. W. MOORE. 1967. Comparison of tetrodotoxin and procaine in internally perfused squid giant axons. *J. Gen. Physiol.* **50**:1413–1428.

QUINCKE. 1861. *Pogg. Ann.* **113**:513. *Cited in* Grahame, D. C. 1947. The electrical double layer and the theory of electrocapilarity. *Chem. Rev.* **41**:441–501.

RUDY, B. 1978. Slow inactivation of the sodium conductance in squid giant axons. Pronase resistance. *J. Physiol. (Lond.)*. **283**:1–21.

SEGAL, J. R. 1968. Surface charge of giant axons of squid and lobster. *Biophys. J.* **8**:470–489.

SHOUKIMAS, J. J. 1978. Effect of calcium upon sodium inactivation in the giant axons of *Loligo pealei*. *J. Membr. Biol.* **38**:271–289.

SHRAGER, P. 1974. Ionic conductance changes in voltage clamped crayfish axons at low pH. *J. Gen. Physiol.* **64**:666–690.

SWENSON, R. P., W. F. GILLY, and C. M. ARMSTRONG. 1981. Absence of charge movement indicates sodium channel inactivation involves silent step. *Proc. VII Int. Biophysics Congress.* Mexico City. 329.

TAKATA, M., W. F. PICKARD, J. Y. LETTVIN, and J. W. MOORE. 1966. Ionic conductance changes in lobster axon membrane when lanthanum is substituted for calcium. *J. Gen. Physiol.* **50**:461–471.

TAYLOR, R. E., C. M. ARMSTRONG, and F. BEZANILLA. 1976. Block of sodium channels by external calcium ions. *Biophys. J.* **16**:27*a*.

TSIEN, R. W. 1974. Effects of epinephrine on the pacemaker potassium current in cardiac Purkinje fibers. *J. Gen. Physiol.* **64**:293–319.

WOODHULL, A. M. 1973. Ionic blockage of sodium channels. *J. Gen. Physiol.* **61**:687–708.